Supplementary Information

Zn Alloying Strategy to Improve Photoluminescence of CuGaS2/ZnS Core/Shell Quantum Dots

Mohammed Abdul Haque[1], Amruta Lohar[1], Yogesh Jadhav[1,2], Ravi Kumar[3], S.N. Jha[4], D. Bhattacharyya[3], Sandesh Jadkar[1], Shrikrishna Sartale[1] and Shailaja Mahamuni[1]*

S1-Synthesis Procedure

In a typical synthesis, 0.0625 mmol of CuI (99.99% Sigma Aldrich), 0.5 mmol of GaI3 (99.99% Sigma Aldrich) and 1 mmol of sulphur (99.9%) were mixed in three-neck flask with 2 mL of 1-dodecanethiol (DDT, ≥98% Sigma Aldrich) and 5 mL of oleylamine (OLA, 70% Sigma Aldrich). The mixture was heated to 120°C with a rate of 20°C per minute under N_2(nitrogen) purging and maintained for 15 min for degassing. Further mixture was heated under N_2 purging to a growth temperature of 240°C. The reaction was maintained at that temperature for 10 min for growth of QDs core. The quaternary ZCGS QDs were synthesized by adding different amount of $ZnCl_2$ (≥98%), 0.5,1.0,1.5 and 2 mmol, corresponding to Zn/Cu precursor molar ratios of 8, 16, and 24 and 32 respectively. The ternary and quaternary core QDs were subjected to the following two step shelling reaction. ZnS stock solution was prepared by dissolving 8 mmol of Zn acetate (reagent grade) in 8 mL of oleic acid (OA, 90%) and 4mL of 1-octadecene (ODE, 90%), by heating the solution to get transparent melt. The hot solution was introduced drop wise using a glass syringe to the core growth solution at 240°C and the reaction was allowed for 75 min. Subsequently, the second ZnS stock solution, consisting of 4 mmol of Zn acetate, 4 mL of OA, 2 mL of DDT, and 2 mL of ODE, was slowly injected, followed by 30 min-reaction at the same temperature. As-reacted QDs were then subjected to the conventional work-up processes of the precipitation with an excess of ethanol and repeated purification with a solvent combination of hexane/ethanol by centrifugation (9000 rpm,10 min), and finally re-dispersed in hexane.

S2- XRD

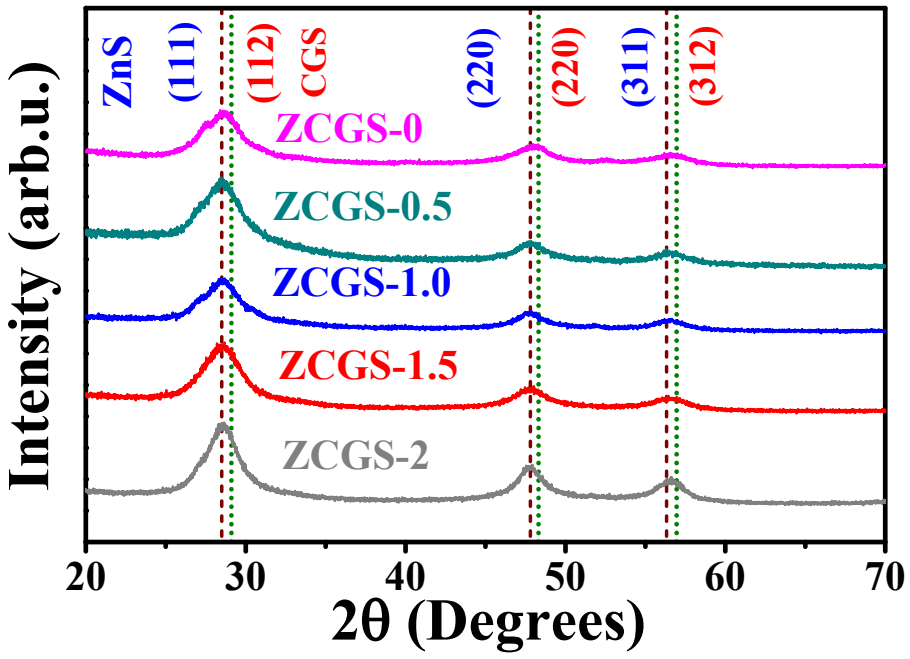

Figure S1 XRD pattern of ternary CGS/ZnS (ZCGS-0) and quaternary ZCGS/ZnS CQDs with varied amount of Zn from 0.5 mmol to 2.0 mmol. The shift of peaks towards zinc blende 2θ values indicate successful ZnS shelling.

S3-TEM

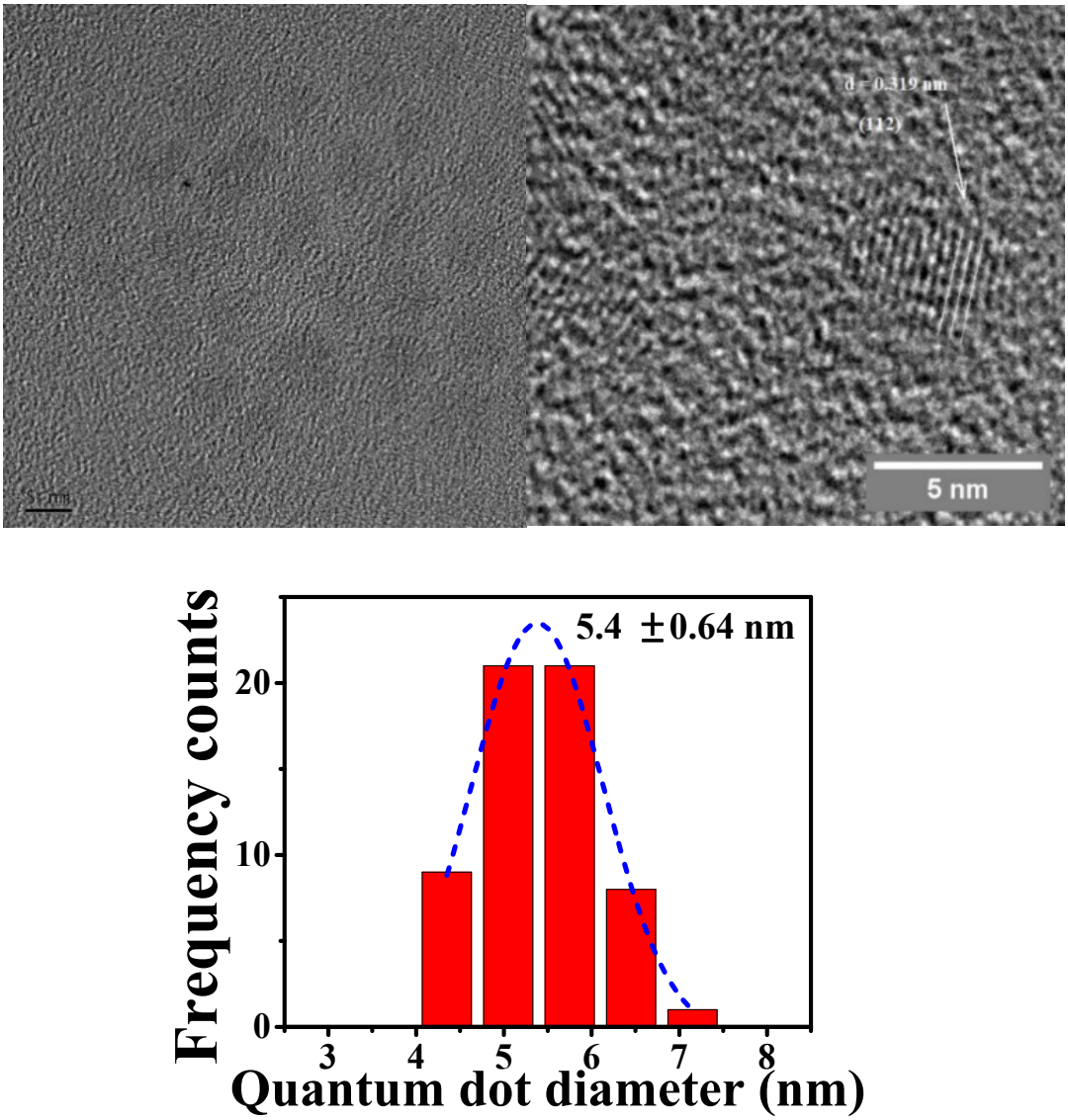

Figure S2 TEM image showing CQDs and with high crystallinity as evident from the visibility of lattice fringes. The d value calculated from adjacent planes is shown in right panel. The histogram for particle size distribution is shown in bottom panel.

S4-Effect of Zn inclusion in the core and of ZnS shell on PL spectrum

To support our conjecture that out of total Zn precursor added to the reaction, a fraction is utilized in cation exchange while the remaining is used up in partial shell formation, here we present the representative core emission spectra of ZCGS-0.5 core showing detectable intensity in contrast to non-emitting core of ternary $CuGaS_2$. This is only possible when surface traps of

the core are passivated by partial ZnS shelling during core growth. Also, dramatic increase in the PL intensity due shell formation can be seen in Figure S3.

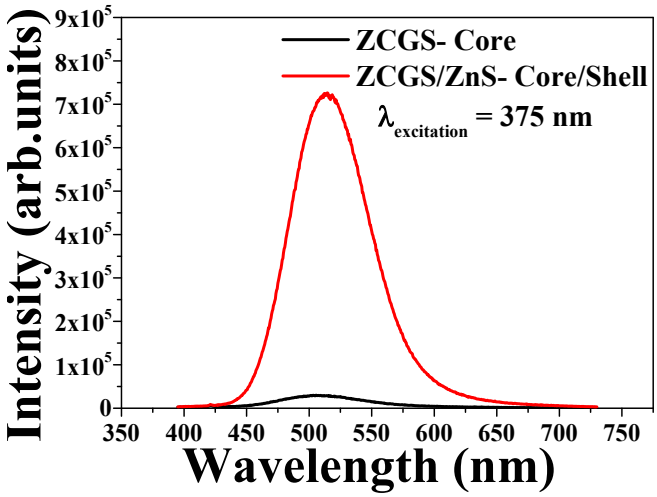

Figure S3 Intensity of ZCGS NCs without shell formation and in core/shell structure at room temperature recorded with excitation wavelength 375 nm. Detectable intensity of ZnCuGaS2 core due to surface passivation by partial shell formation during core growth

S5-Stability of QDs

The $CuGaS_2$/ZnS core-shell quantum dots (QDs) achieve enhanced stability through several mechanisms. The ZnS shell serves as a protective barrier, passivating the QD surface to prevent oxidation and degradation of the $CuGaS_2$ core material. Additionally, the shell reduces surface defects, minimizing sites for chemical reactions and enhancing the

stability. It also provides improved colloidal stability by steric hindrance and electrostatic repulsion, preventing QD aggregation in solution. Also, the ZnS shell offers protection against external factors like moisture and contaminants, preserving the optical and electronic properties of $CuGaS_2$/ZnS QDs over time. As an example, please refer to the following Figure S4 showing photograph of powdered samples stored in open environment showing bright luminescence under illumination with UV lamp.

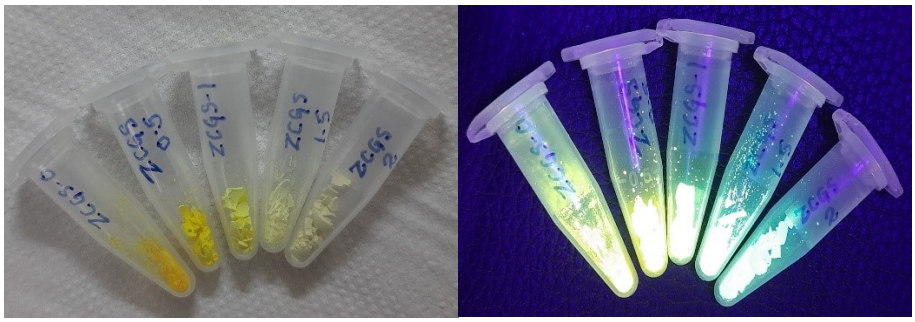

Figure S4 powdered samples under room light (left panel) and under UV illumination

(right panel)

The graded interface, resulting from Zn diffusion during core synthesis and shelling, promotes radiative recombination by minimizing surface defects and gradually relaxing strain. The broad PL observed for our ZCGS/ZnS samples with a full width at half maximum (FWHM) of 350 meV primarily stems from the graded composition at the interface between the $CuGaS_2$ core and ZnS shell in the QDs. The composition gradient, creates energy states of varying depths within the QD structure, significantly influencing the observed broad PL spectrum. The epitaxial shell growth due to nearly same lattice parameters of chalcopyrite core and ZnS shell results in effective passivation of surface defects and enhances the emission intensity. Hence the sample showing most bright luminescence implies effective surface passivation and hence will also be most stable one.

S6-Cyclic Voltammetry

A glassy carbon electrode (GCE), silver wire, and platinum wire loop were used as working, quasi reference, and counter electrodes, respectively. The electrodes were precleaned with dilute nitric acid. The working electrode was polished with 0.5 μm Al_2O_3 powder and washed with an excess of DI water a few times to remove any contamination. Tetrabutylammonium perchlorate (TBAP-100 mM) dissolved in dichloromethane (DCM-10 mL) was used as supporting electrolyte. The potentials were calibrated and presented with respect to NHE using ferrocene standard.[1] The controlled experiments were performed in TBAP- DCM mixture, on a bare electrode (without any sample). The CV measurements were performed by drop casting 30 μL of ZCGS CQDs-hexane dispersion on the GCE followed by vacuum drying.

S7-X-ray Absorption Spectroscopy of $CuGaS_2$ (CGS) quantum dots coated with ZnS

X-ray Absorption Spectroscopy (XAS) measurements, which comprises of both X-ray Near Edge Structure (XANES) and Extended X-ray Absorption Fine Structure (EXAFS)techniques, have been carried out to probe the local structure of $CuGaS_2$ (CGS) quantum dots coated with ZnS. The XAS measurements have been carried out at the Energy-Scanning EXAFS beamline (BL-9) at the Indus-2 Synchrotron Source (2.5 GeV, 100 mA) at Raja Ramanna Centre for Advanced Technology (RRCAT), Indore, India.[2,3] This beamline operates in the energy range of 4 KeV to 25 KeV. The beamline optics consists of a Rh/Pt coated collimating meridional cylindrical mirror and the collimated beam reflected by the mirror is monochromatized by a Si

(111) (2d=6.2709 Å) based double crystal monochromator (DCM). The second crystal of DCM is a sagittal cylinder used for horizontal focusing while a Rh/Pt coated bendable post mirror facing down is used for vertical focusing of the beam at the sample position. Rejection of the higher harmonics content in the X-ray beam is performed by detuning the second crystal of DCM. In the present case, XAS measurements have been performed in the transmission mode at Zn K edge and in the fluorescence mode at Cu K edge.

For the transmission mode measurement, three ionization chambers (300 mm length each) have been used for data collection, one ionization chamber for measuring incident flux (I_0), second one for measuring transmitted flux (I_t) and the third ionization chamber for measuring XAS spectrum of a reference metal foil for energy calibration. Appropriate gas pressure and gas mixtures have been chosen to achieve 10-20 % absorption in first ionization chamber and 70-90% absorption in second ionization chamber to improve the signal to noise ratio. The absorption coefficient μ is obtained using the relation:

$$I_T = I_0 e^{-\mu x} \qquad (1)$$

where, x is the thickness of the absorber.

For measurements in the fluorescence mode, the sample is placed at 45° to the incident X-ray beam, and a fluorescence detector is placed at right angle to the incident X-ray beam to collect the signal. One ionization chamber detector is placed prior to the sample to measure the incident flux (I_0) and florescence detector measures the fluorescence intensity (I_f). In this case the X-ray absorption co-efficient of the sample is determined by $\mu = I_f / I_0$, and the spectrum was obtained as a function of energy by scanning the monochromator over the specified range

To obtain the qualitative information about the local structure, oscillations in the absorption spectra $\mu(E)$ have been converted to absorption function $\chi(E)$ defined as follows:

$$\chi(E) = \frac{\mu(E) - \mu_0(E)}{\Delta\mu_0(E_0)} \qquad (2)$$

where, E_0 is absorption edge energy, $\mu_0(E_0)$ is the bare atom background and $\Delta\mu_0(E_0)$ is the step in $\mu(E)$ value at the absorption edge. The energy dependent absorption coefficient $\chi(E)$ has been converted to the wave number dependent absorption coefficient $\chi(k)$ using the relation,

$$K = \sqrt{\frac{2m(E - E_0)}{\hbar^2}} \qquad (3)$$

where, m is the electron mass. $\chi(k)$ is weighted by k^2 to amplify the oscillation at high k and the $\chi(k)k^2$functions are Fourier transformed in R space to generate the $\chi(R)$ versus R spectra in terms of the real distances from the center of the absorbing atom. The set of EXAFS data analysis program available within Demeter software package has been used for EXAFS data analysis. This includes background reduction and Fourier transform to derive the $\chi(R)$ versus R spectra from the absorption spectra (using ATHENA software), generation of the theoretical EXAFS spectra starting from an assumed crystallographic structure and finally fitting of experimental data with the theoretical spectra using ARTEMIS software.[4]

Cu K-edge

The normalized absorption spectra of all samples at Cu-K edge are shown in Figure S5. $\chi(R)$ versus R plots at Cu K-edge are generated by Fourier transform of $k^2\chi(K)$ vs. k spectra (Figure S6) following the methodology described above over k range of 3.0-9.5Å^{-1}and are shown in Figure S7. We have fitted the EXAFS data of all samples in the range of 1.2-2.6 Å in R space. The scattering paths have been generated from the $CuGaS_2$ crystal structure. The first peak at 1.9 Å has contribution from Cu-S coordination shell. The best fit parameters are shown in table I.

Table I: Bond length, coordination number and disorder factors obtained by EXAFS fitting measured at Cu K- edge.

Path	Parameter	ZCGS-0.5	ZCGS-1	ZCGS-1.5	ZCGS-2
Cu K edge					
Cu-S	R (Å) (2.31)	2.33 ±0.01	2.31 ±0.01	2.32 ±0.01	2.28 ±0.01
	N (4)	4.0±0.12	4.0±0.16	4.0±0.08	4.0±0.08
	σ^2	0.0063± 0.0006	0.0079± 0.0009	0.0069± 0.0004	0.006± 0.0004
	R_{factor}	0.005	0.01	0.002	0.004

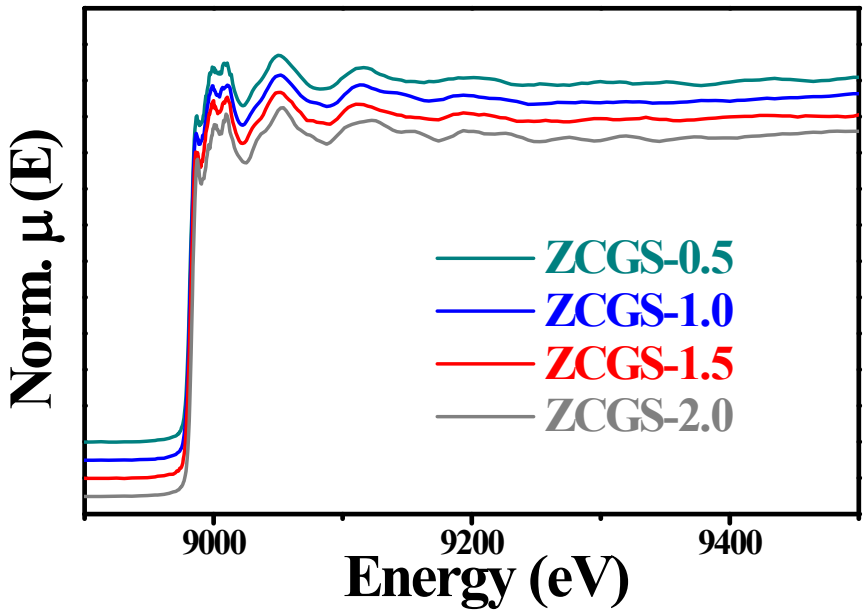

Figure S5 Normalized XAS spectra of $CuGaS_2$ (CGS) quantum dots coated with ZnS measured at Cu K-edge

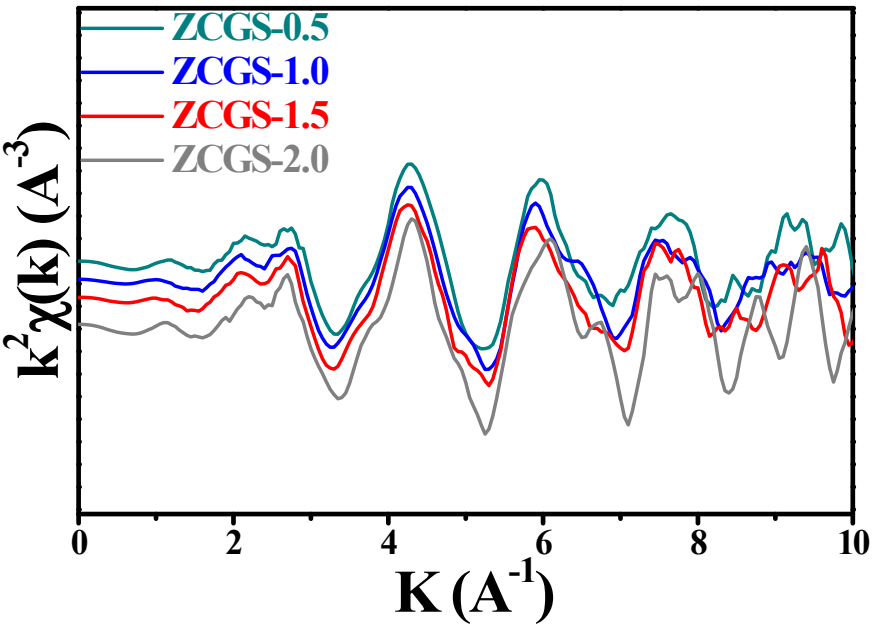

Figure S6 EXAFS ($k^2\chi$(k) Vs k) of $CuGaS_2$ (CGS) quantum dots coated with ZnS measured at Cu K-edge

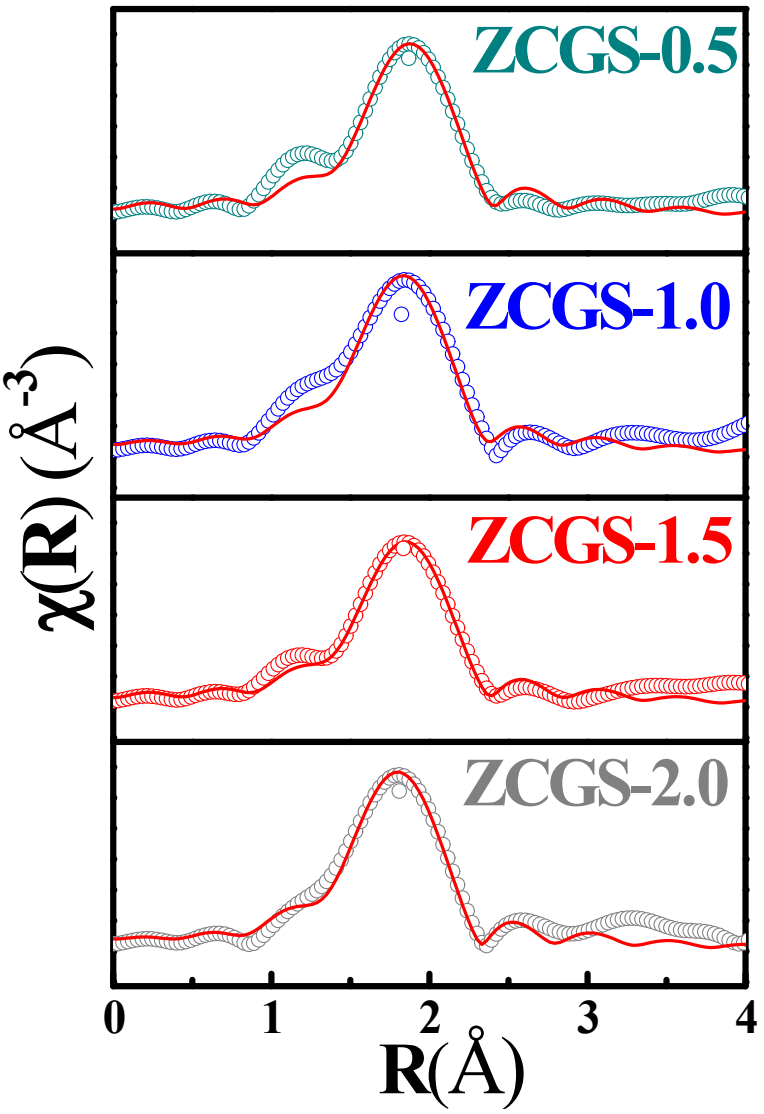

Figure S7 Fourier transformed EXAFS of $ZnCuGaS_2$ (ZCGS) CQDs coated with ZnS at Cu K-edge. The experimental spectra are represented by scatter points and theoretical fits are represented by solid lines

Reported value of Cu-S bond length is 2.31 $Å^4$ in CuGaS2 which is close to the observed value. Zn incorporation in $GuGaS_2$ is not causing any distortion. This may be since ionic radius of Cu and Zn are almost same.

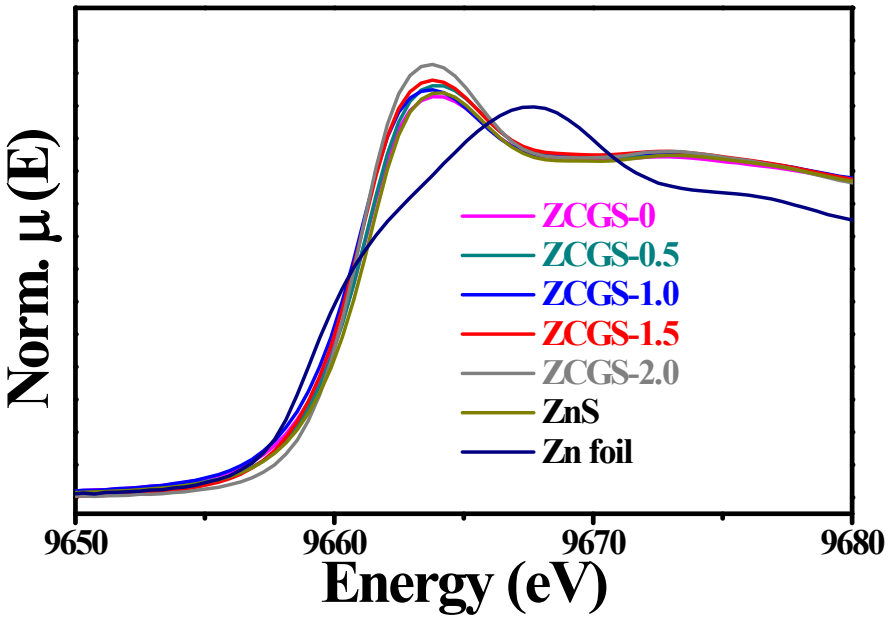

Figure S8 Normalized XANES spectra of $CuGaS_2$ (CGS) quantum dots coated with ZnS along with Zn foil and ZnS measured at Zn K-edge

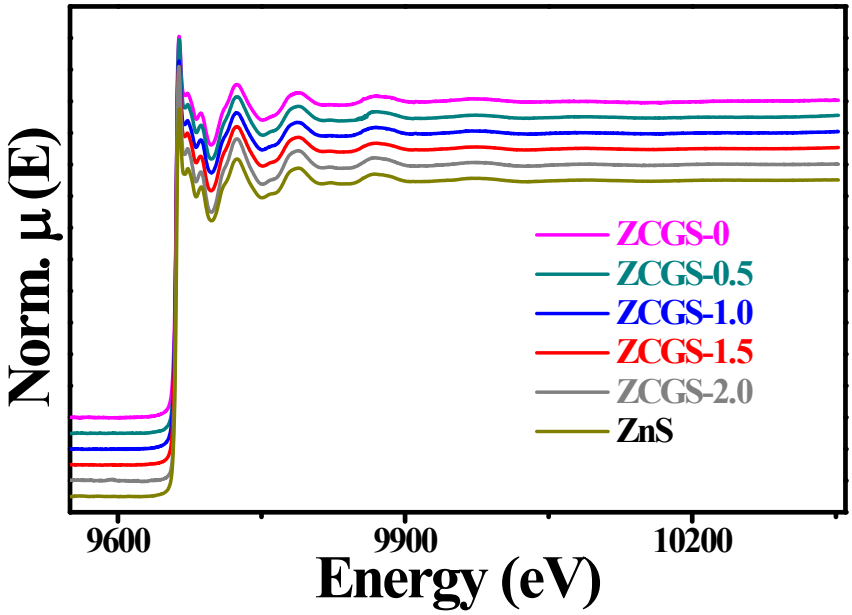

Figure S9 Normalized XAS spectra of $CuGaS_2$ (CGS) quantum dots coated with ZnS along with ZnS measured at Zn K-edge

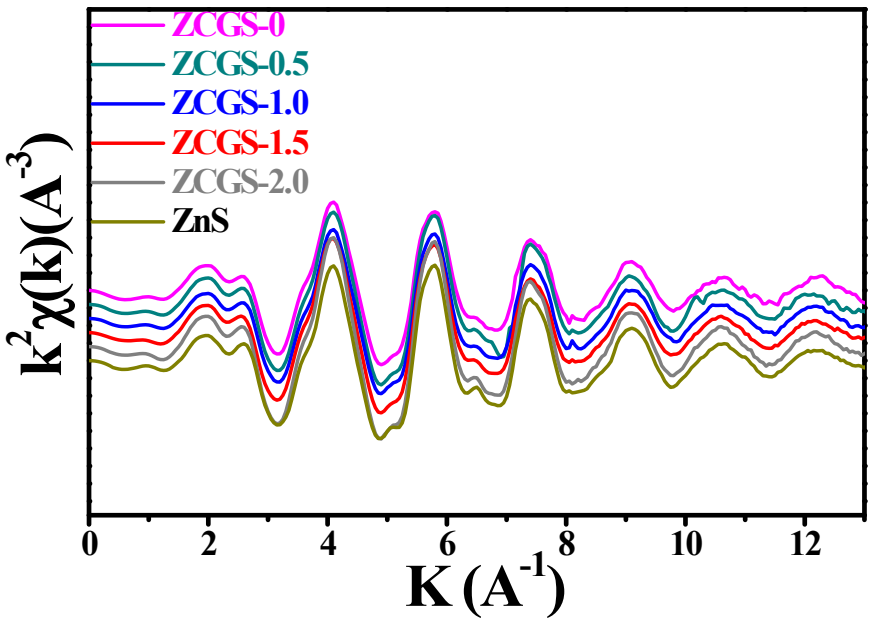

Figure S10 EXAFS ($k^2\chi$(k) Vs k) of $CuGaS_2$ (CGS) quantum dots coated with ZnS along with ZnS measured at Zn K-edge

Reference:

(1) Maiti, S.; Dana, J.; Jadhav, Y.; Debnath, T.; Haram, S. K.; Ghosh, H. N. Electrochemical Evaluation of Dopant Energetics and the Modulation of Ultrafast Carrier Dynamics in Cu-Doped CdSe Nanocrystals. *J. Phys. Chem. C* **2017**, *121* (48), 27233–27240. https://doi.org/10.1021/acs.jpcc.7b10262.

(2) Basu, S.; Nayak, C.; Yadav, A. K.; Agrawal, A.; Poswal, A. K.; Bhattacharyya, D.; Jha, S. N.; Sahoo, N. K. A Comprehensive Facility for EXAFS Measurements at the INDUS-2 Synchrotron Source at RRCAT, Indore, India. *J. Phys. Conf. Ser.* **2014**, *493* (1), 3–7. https://doi.org/10.1088/1742-6596/493/1/012032.

(3) Poswal, A. K.; Agrawal, A.; Yadav, A. K.; Nayak, C.; Basu, S.; Kane, S. R.; Garg, C. K.; Bhattachryya, D.; Jha, S. N.; Sahoo, N. K. Commissioning and First Results of Scanning Type EXAFS Beamline (BL-09) at INDUS-2 Synchrotron Source. *AIP Conf. Proc.* **2014**, *1591*, 649–651. https://doi.org/10.1063/1.4872706.

(4) Newville, M.; Ravel, B.; Haskel, D.; Rehr, J. J.; Stern, E. A.; Yacoby, Y. Analysis of Multiple-Scattering XAFS Data Using Theoretical Standards. *Phys. B Phys. Condens. Matter* **1995**, *208–209* (C), 154–156. https://doi.org/10.1016/0921-4526(94)00655-F.